Sains Malaysiana 37(2)(2008): 131-135

Surface Analysis of Marine Sulphate-Reducing Bacteria Exopolymers on Steel During Biocorrosion Using X-ray Photoelectron Spectroscopy

(Analisis Permukaan Eksopolimer Bakteria Penurun-Sulfat Marin pada Keluli Semasa Kakisan Bio Menggunakan Spektroskopi Fotoelektron Sinar-X)

FATHUL KARIM SAHRANI, MADZLAN ABD. AZIZ, ZAHARAH IBRAHIM & ADIBAH YAHYA

ABSTRACT

The aim of this study was to determine the surface chemistry during biocorrosion process on growth and on the production of exopolymeric substances (EPS) in batch cultures of mix-strains of marine sulphate-reducing bacteria (SRB) isolated from Malaysian Shipyard and Engineering Harbour, Pasir Gudang. The EPS and precipitates were analyzed by X-ray photoelectron spectroscopy (XPS). The XPS results indicate that Fe($2p_{3/2}$) spectrum for iron sulphide can be fitted with Fe(II) and Fe(III) components, both corresponding to Fe-S bond types. The absence of oxide oxygen in the O(1s) spectrum and Fe(III)-O bond types in the Fe($2p_{3/2}$) spectrum supports the conclusion that iron sulphides are composed of both ferric and ferrous iron coordinated with monosulphide and disulphide.

Keywords: Sulphate-reducing bacteria; biocorrosion; exopolymeric substances; X-ray photoelectron spectroscopy

ABSTRAK

Tujuan kajian ini adalah untuk menentukan keadaan kimia permukaan semasa proses kakisan bio terhadap pertumbuhan dan penghasilan bahan eksopolimer (EPS) dalam campuran pengkulturan bakteria penurun sulfat marin yang dipencilkan daripada Kejuruteraan Berat dan Marin Malaysia Sdn. Bhd. (MHHE), Pasir Gudang. EPS dan mendakan pada permukaan keluli dianalisis menggunakan spektroskopi fotoelektron sinar-X (XPS). Analisis menggunakan XPS menunjukkan spektrum Fe($2p_{3/2}$) untuk besi sulfida boleh dipadankan kepada komponen Fe(II) dan Fe(III), sepadan kepada jenis ikatan Fe-S. Ketiadaan oksigen oksida dalam spektrum O(1s) dan jenis ikatan Fe(III)-O dalam spektrum Fe($2p_{3/2}$) menyokong kesimpulan bahawa besi sulfida mengandungi kedua-dua besi ferik dan ferus serupa dengan monosulfida dan disulfida.

Kata kunci: Bakteria penurun-sulfat; kakisan bio; bahan eksopolimer; spektroskopi fotoelektron sinar-X

INTRODUCTION

In marine environments, the growth of biofilms harbouring sulfate-reducing bacteria (SRB) on steel structures often results in severe corrosion damage of the material (Cheung et al. 1994; Gubner & Beech 1996; Odom & Singleton 1992). Several theories have been proposed to explain possible mechanisms by which SRB can influence the deterioration of steel (Hamilton 1985; Lee et al. 1995). Few reports, however, examine the role of the SRB extracellular polymeric substances (EPS) in this process (Beech & Gaylarde 1991; Beech et al. 1999). The binding of metal ions by bacterial EPS, including exopolymers secreted by SRB, is well documented (Beech & Cheung 1995; Ford et al. 1988; Geesey & Jang 1985) and metal ion chelating properties of EPS have been proposed as the main reason for the ability of exopolymer to influenced the corrosion reaction (Little et al. 1990).

The SRB secrete various organic substances such as extracellular polymer substances, primarily composed of polysaccharides, uronic acid sugars and proteins, containing functional groups such as carboxylic acid and amino acid groups, which could be acidic and capable of binding metal ions (Gaylarde & Videla 1995). The metal ion chelating properties of EPS have been reported as a mechanism of corrosion (Beech & Cheung 1995). It has also been suggested that iron oxides, as a source of ferrous ions, can be dissolved reductively by reacting with abiotic hydrogen sulphide and be transformed into sulphides in the presence of SRB. SRB can dissimilatorily reduce sulphate to sulphide ions; biogenic hydrogen sulphide and iron sulphides (FeS_x) formed by the precipitation of ferrous ions with the sulphide ions acting as a cathode in galvanic couple can enhance corrosion (Duan et al. 2006).

The X-ray photoelectron spectroscopy (XPS) has been used to investigate microorganisms, proteins and microbial adhesions on metallic and non-metallic surfaces (Baty et al. 1996; Beech et al. 1999; Sosa et al. 1994). Although XPS is often employed to study bonding in metal compounds, its application in the field of metal ion-microbial exopolymer interaction has been limited. The technique has limited ability to provide detailed molecular information, particularly when atoms are in a wide variety of chemical states, as is the case for macromolecules, such as carbohydrates and proteins. However, the presence of

biogenic corrosion products especially sulphides on the surfaces detected using XPS can be used as an evidence to the role of SRB in biocorrosion process.

EXPERIMENTAL DETAILS

Carbon-low alloys steel (4100 Series) cylindrical coupons (9.5 mm diameter × 6.0 mm) were polished with 0.3 micron alumina paste to a mirror finish, washed with distilled water and ethanol and stored in desiccators. The coupons were marked on the bottom and wiped with ethanol. The three days culture of SRBI and SRBII were isolated and grown overnight at ± 37°C in VMNI medium (patent name for SRB growth) containing coupons. The experiments were carried out under two conditions: (1) VMNI (control) and (2) VMNI + SRB1 + SRB11.

The culture and coupons were incubated for 72 hours before they were removed and air-dried without rinsing. XPS spectra were recorded with an AXIS 165 electron spectrometer by Kratos Analytical, using monochromatic AlK_{μ} radiation at 100W at the Materials Science Programme laboratory, Universiti Kebangsaan Malaysia. The air-dried samples were mounted on UHV-resistant tape and evacuated for several hours to stabilize the water content in the organic surface films (Johansson & Saastamoinen 1999). Wide binding energy range spectra (0-1100 eV) were recorded using 80 eV pass energy and 0.5 eV steps. The high-resolution spectra of C_{1s}, O_{1s}, Fe_{2p}, N_{1s} and S_{2p} regions were recorded using 20 eV pass energy and 0.2 eV steps. Wide subsurface spectra were also recorded after 2 minutes of Ar^{+} ion sputtering. Subsurface high-resolution measurements were not recorded, as sputtering tends to destroy the chemical structure in organic compounds and metal oxides. The analyzed area was about 1 mm and the pressure in the analysis chamber was below 9×10^{-9} torr during the data acquisition (Briggs 1997; Briggs & Seah 1990).

RESULTS AND DISCUSSION

The narrow region spectrum for C (1s) (coupons in VMNI inoculated with SRB1 and SRB11) indicates a prominent peak with a quite large shoulder on high binding energy limb (Figure 1a). All peaks were corrected at 284.5 eV with the charging effect ± 1.22 eV as advantages carbon or C_{α}-terminal. (Moulder et al. 1992; Stipp & Hochella 1991).

Four other components are fitted at 286.03eV, 287.89eV and 283.16eV and 289.81 eV (Table 1), representing as alcohol/ether, aldehyde/ketone, hydrocarbon and carboxyls bond types, respectively (Clack & Thomas 1978; Herbert et al. 1998; Mathez 1987). While the hydrocarbon peak is adventitious (as the hydrocarbon peak appears at lower binding energy of 285.0 eV), C in alcohol and aldehyde bond types would be components from bacterial cellular membranes, similar XPS peak positions were reported by Wolf and Ferris (1995) for biofilms recovered from neutral pH surface water. Growth of SRB on the coupon leads to a change of the C (1s) signal shape compared to control (Figure 1a), ascribed to an increase of the contribution both from C–N (287.9 eV) and oxidized works (Mishra & Weimer, 1997; Xiao et al. 1997). It is in good agreement with N (1s) peak presence

TABLE 1. Binding energies (E_b), peak full at half maximum (FWHM) and peak areas for C (1s) narrow region scans of photoelectron spectrum

Peaks	FWHM (eV)	Mass (%) concentration	Remarks
C (1s) 1	1.44	54.10	carbon-α
C (1s) 2	1.44	19.73	alcohol/ether
C (1s) 3	1.44	14.26	aldehyde/ketone
C (1s) 4	1.44	7.42	hydrocarbon
C (1s) 5	1.44	4.49	carboxyls

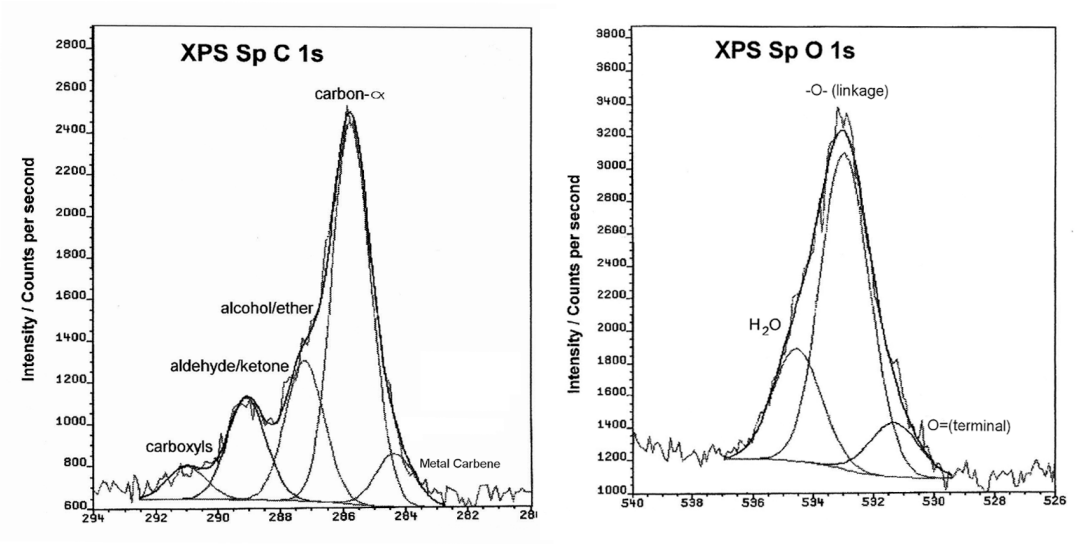

(a) (b)

FIGURE 1. Narrow region scans of (a) C (1s) and (b) O (1s)

that is observed only for coupon after exposed in SRB cultures (Figure 3).

The O (1s) spectrum is broad FWHM of 1.9 eV (see Figure 1b) and is best fitted with three peaks at 531.35, 532.49 and 533.67eV (Table 2). The lowest O (1s) binding energy peak is attributable to terminal oxygen (O=) which probably due to hydroxyl groups in organic compounds found in bacterial cells. The remaining higher binding energy peaks correspond to linkage oxygen (-O-). While both peaks are in the binding energy range for adsorbed water (Harvey & Linton 1981), the higher binding energy peak (533.67 eV) may actually correspond to several components including residual cellular water. It should be noted that no oxide oxygen could be fitted to the data, as the oxide oxygen peak appears at lower binding energies, 530.0 eV in goethite (Ferris et al. 1989) and would fall at the beginning of the low binding energy shoulder for the O (1s) peak (see Figure 1b).

As shown in Figure 2a, each surface species in the Fe (2p) spectrum is fitted with a double representing the spin-orbit splitting of the Fe ($2p_{1/2}$) and Fe ($2p_{3/2}$) peaks. The Fe ($2p_{3/2}$) photoelectron spectrum is very broad, (FWHM, 2.8 eV (Figure 2a) and resembles the Fe ($2p_{3/2}$) spectrum presented by Pratt et al. (1994) for vacuum-fracture pyrrhotite, although with a somewhat smaller FWHM. Prat et al. (1994) fitted their spectrum with both as Fe(II) and Fe(III) components, both corresponding to iron-sulfur bond types, which was interpreted as the structural incorporation of Fe^{2+} and Fe^{3+} in the pyrrhotite lattice. The approach of Pratt et al. (1994) is followed in this study and the Fe $2p_{3/2}$ spectrum is fit with only Fe^{2+} single peak (Table 3); the primary Fe^{2+} peak in the binding energy range reported for Fe(II) bounded to S (Mycroft et al. 1990; Prat et al. 1994).

The Fe ($2p_{3/2}$) spectrum is too broad to be fitted solely with the Fe^{2+} single peaks and another component needs to be fitted to the high binding energy side of the peak. The presence of the oxidized surface species is possible, owing to brief exposures to atmospheric oxygen during sample handling. However, peaks with binding energies attributable to Fe(III)–O bonds in oxides and hydroxides (e.g. hematite; goethite) appear at higher binding energies, (710.0 to 713.0 eV) (Herbert et al. 1998) and cannot be fitted well to the data; in addition, oxide oxygen was not detected in the O (1s) spectrum. The Fe $2p_{3/2}$ spectrum is best fitted as Fe(III) component with a binding energy in the range of Fe(III)–S bond types. As with pyrrhotite (Pratt et al. 1994), this Fe(III) component is modeled in a high spin state with two multiple peaks; the primary peak at 710.1 eV and the remaining with the higher binding energy 712.9 eV is constrained to the same shape. From this data, it appears that Fe(III) is coordinated with reduced sulfur at the sulfide surface and is a structural component, as in pyrrhotite (Pratt et al. 1994) or greigite (Fe_3S_4) (Duan et al. 2005).

Figure 3 shows the narrow region scan for S (2p) which run from 158.0 to 170.0 eV. In this spectrum, 60% of the S (2p) signal is fitted with a peak binding energy of 160.9 eV which is somewhat lower than typical S (2p) binding energies for iron monosulphides such as pyrrhotite (e.g. 161.1 eV by Jones et al. 1992; 161.2 eV by Pratt et al. 1994). Additionally, disulphide (S_2^{2-}) species are fitted to

TABLE 2. Binding energies (E_b), peak full at half maximum (FWHM) and peak areas for O (1s) narrow region scans of photoelectron spectrum

Peak	FWHM (eV)	Mass (%) concentration	Remarks
O (1s) 1	1.90	65.61	O= (terminal)
O (1s) 2	1.90	23.28	-O- (linkage)
O (1s) 3	1.90	11.11	H_2O

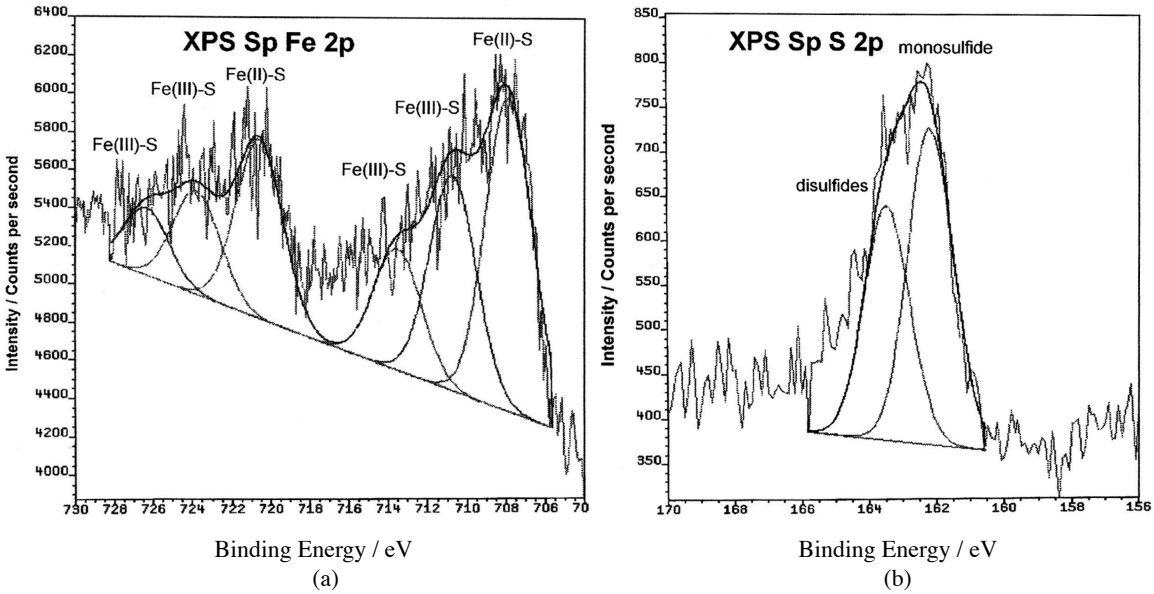

FIGURE 2. Narrow region scans of (a) Fe (2p) and (b) S (2p)

TABLE 3. Binding energies (E_b), peak full at half maximum (FWHM) and peak areas for Fe (2p) narrow region scans of photoelectron spectrum

Peak	FWHM (eV)	Mass concentration (%)	Remarks
Fe (2p) 1	2.82	31.39	Fe(II)–S from Fe ($2p_{3/2}$)
Fe (2p) 2	2.82	17.87	Fe(II)–S from Fe ($2p_{1/2}$)
Fe (2p) 3	2.82	21.59	Fe(III)–S from ($2p_{3/2}$)
Fe (2p) 4	2.82	10.30	Fe(III)–S from Fe ($2p_{1/2}$)
Fe (2p) 5	2.82	12.16	Fe(III)–S from ($2p_{3/2}$)
Fe (2p) 6	2.82	6.69	Fe(III)–S from Fe ($2p_{1/2}$)

TABLE 4. Binding energies (E_b), peak full at half maximum (FWHM) and Peak areas for S (2p) narrow region scans of photoelectron spectrum

Peak	FWHM (eV)	Mass concentration (%)	Remarks
S (2p) 1	1.58	59.93	monosulfides
S (2p) 2	1.58	40.07	disulfide

Table 5. Binding energies (E_b), peak full at half maximum (FWHM) and peak areas for N 1s narrow region scans of photoelectron spectrum

Peak	FWHM (eV)	Mass concentration (%)	Remarks
N (1s) 1	1.84	100	organic matrix

the data at the 163.16 eV binding energy, the sum of these species totals 40%. In organo-sulphur compounds such as proteins, most S (2p) binding energies range between 162.0 to 167.0 eV, indicating that sulphur may be organically bound in cell membranes (Moulder et al. 1992). Although the S (2p) spectrum has been fitted with disulfide, the high binding energy tail to the S 2p spectrum could instead be fitted with a range of organic-S compounds representing protein in bacterial membranes.

The N (1s) spectrum is broad (Figure 3) and could be fitted to a single peak with the binding energy 400.25 eV (Table 5). The N (1s) binding energy peak is corresponding to organic matrix which in range between 398.8 to 401 eV (Moulder et al. 1992). After exposed of sample in the SRB culture, a new peak of bonded nitrogen, N (1s) at 400.25 eV appears which is associated with formation of thin adsorbed protein layer on metal surface (Pradier et al. 2000; Xiao et al. 1997). As described in the literature, it could be formed by superposition of contribution from amides (400.0 eV) (Mishra & Weimer 1997; Xiao et al. 1997).

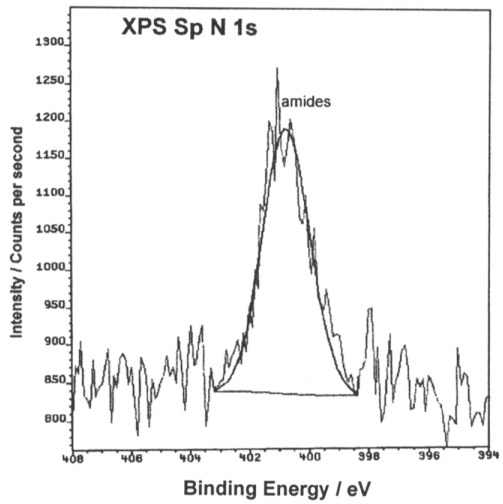

FIGURE 3. Narrow region scans of N_{1s}

CONCLUSION

This study was able to determine the formation of iron sulphide on steel surface during biocorrosion as a results of SRB activities. The presence of signal N (1s) in photoelectron spectrum indicated as biofilm (EPS) was presented on the sample which exposed in SRB culture. The lack of oxide oxygen in the O (1s) spectrum and the absence of Fe(II)–O and Fe(III)–O bond types in the Fe ($2p_{3/2}$) spectrum supports the conclusion that the poorly crystalline iron sulphide formed in this study is composed of both ferric and ferrous iron coordinated with mono and disulphide for exposed stainless steel in SRB culture. The results implied that SRB activities could be partly responsible for the reduction of metal oxides and the formation of sulphide species.

ACKNOWLEDGEMENT

We wish to acknowledge the facilities given by Malaysian Shipyard and Engineering Sdn. Bhd., Pasir Gudang, Johor and UKM-JPA for their generous financial support throughout the study.

REFERENCES

Baty, A.M., Suci, P.A. Tyler, B.J. & Geesey, G.G. 1996. Investigation of mussel adhesin protein adsorption on polystyrene and polyoctadecyl methacrylate using angle dependent XPS, ATR-FTIR AFM. *J. Colloid Interface Sci.* 177: 307-315.

Beech, I.B. & Cheung, C.W.S. 1995. Interactions of exopolimers produced by sulphate-reducing bacteria with metal ions. *Int. Biodet. Biodeg*. 35: 59-72.

Beech, I.B. & Gaylarde, C.C. 1991. Microbial polysaccharides and corrosion. *Int. Biodet*. 27: 95-107.

Beech, I.B., Zinkevich, V., Tapper, R., Gubner, R. & Avei, R. 1999. Study of the interaction of sulphate-reducing bacteria exopolimers with iron using X-ray photoelectron spectroscopy and time-of-flight secondary ionization mass spectrometry. *J. Microbiol. Methods*. 36: 3-10.

Briggs, D. 1997. *Surface Analsis of Polymers by XPS and Static SIMS*. Cambridge: Cambridge University Press.

Briggs, D. & Seah, M.P. 1990. *Auger and X-ray photoelectron Spectroscopy, in practical surface analysis*. Chichester, England: John Wiley & Sons Inc.

Cheung, C.W.S., Wals, F.C. Chun, V., Campbell, S.A. & Beech, J.B. 1994. The role of microbial consortia in marine corrosion of carbon steel. *Int. Biodet. Biodeg*. 34 (3-4): 259-279.

Clark, D.T. & Thomas, H.R. 1978. Applications of ESCA to polymer chemistry, XVII, Systematic investigation of the core levels of simple homo-polymers inpure oxygen and helium-oxygen mixtures. *J. Polym. Sci. Polym. Chem*. Eds. 17: 967-976.

Duan, J., Hou, B. & Yu, Z. 2006. Characteristics of sulfide corrosion products on 316L stainless steel surfaces in the presence of sulfate-reducing bacteria. *Materials Science and Engineering* C 26: 624-629.

Ferris, F.G., Tazaki, K. & Fyfe, W.S. 1989. Iron oxides in acid mine drainage environments and their association with bacteria. *Chem. Geol*. 74: 321-330.

Ford, T.E., Maki, J.S. & Mitchell, R. 1988. Involvement of bacterial exopolymers in biodeterioration of metals. In *Biodeterioration 7*, Houghton, D.R., Smith, R.N., Eggins, H.O.W. (eds.). Proceedings of the Seventh International Biodeterioration Symposium. Barking Essex, U.K.: Elsevier Applied Science. 378-384.

Gaylarde, C.C. & Videla, H.A. 1995. *Bioextraction and Biodeterioration of metals*. Cambridge: Cambridge University Press.

Geesey, G.G. & Jang, L. 1985. Extracellular polymers for metal binding. In *Microb. Mineral Recovery*. McGraw-Hill: 223-247.

Gubner, R. & Beech, I.B. 1996. Field and laboratory studies of marine biocorrosion of carbon steel. *Proceedings of tne 2nd NACE Latin American Congress on Corrosion*, 9-13 September 1996, Rio de Janeiro, Brazil. NACE International Electronic Publication, Paper LA 9: 61-75.

Hamilton, W.A. 1985. Sulfate-reducing bacteria and anaerobic corrosion. *Ann. Rev. Microbiol*. 39:195-217.

Harvey, D.T. & Linton, R.W. 1981. Chemical characterization of hydrous ferric oxides by x-ray photoelectron spectroscopy. *Anal. Chem*. 53: 1648-1688.

Herbert, R.B., Benner, S.G., Pratt, A.R. & Blowes, D.W. 1998. Surface chemistry and morphology of poorly crystalline iron sulfides precipitated in media containing sulfate-reducing bacteria. *Chemical Geology* 144: 87-97.

Johansson, L.-S. & Saastamoinen, T. 1999. Investigating early stages of biocorrosion with XPS: AISI 304 stainless steel exposed to *Burkholderia* species. *Appl. Surf. Sci*. 92: 144–145.

Jones, C.F., Lecount, S., Smart, R. St. C. & White, T. 1992. Compositional and structural alteration of pyrrhotite surfaces in solution: XPS and XRD studies. *Appl. Surf. Sci*. 55: 65-85.

Lee, W., Lewandowski, Z., Nielson, P.H. & Hamilton, W.A. 1995. Role of sulphate-reducing bacteria in corrosion of mild steel: A review. *Biofouling* 8:165-194.

Little, B.J., Wagner, P.A., Characklis, W.G. & Lee, W. 1990. Microbial Corrosion. In *Biofilms*, Characklis, W.G. & Marshall, K.C. (eds.). New York: Wiley, pp. 635-670.

Mathez, E.A. 1987. Carbonaceous matter in mantle xenoliths: composition and relevance to the isoltopes. *Geochim. Cosmochim. Acta*. 51: 2339-2347.

Mishra, S. & Weimer, J.J. 1997. The iron oxides, structure and properties. In *Proceedings of the 23rd Annual Meeting of the Society of Biometerials*, New Orleans, USA, April 1997.

Moulder, J.F., Stickle, W.F., Sobol, P.E. & Bomben, K.D. 1992. *Handbook of X-ray Photoelectron Spectroscopy*. Perkin-Elmer Corporation, Physical Electronics Division. United States of America.

Mycroft, J.R., Brancroft, G.M., McIntyre, N.S., Lorimer, J.W. & Hill, I.R. 1990. Detection of sulphur and polysulphides on electrochemically oxidised pyrite surfaces by x-ray photolectron spectroscopy and Raman spectroscopy. *J. Electroanal. Chem*. 292: 139-152.

Odom, J.M. & Singleton, R. 1992. *The Sulfate-reducing bacteria: Contemporary perspectives*. New York: Springer-Verlag.

Pradier, C.M., Bertrand, P., Bellon-Fontaine, M.N., Costa, D., Marcus, P., Poleunis, C., Rondot, B. & Walls, M.G. 2000. AFM and XPS probing of stainless steel surfaces subjected to biological influences. *Surf. Interf. Anal*. 30: 45-56.

Pratt, A.R., Muir, I.J. & Nesbitt, H.W. 1994. X-ray photoelectron and Auger Spectroscopic studies of Pyrrhotite and Mechanism of air oxidation. *Geochim. Cosmochim. Acta* 58: 227-841.

Sosa, R.C., Masy, D. & Rouxhet, P.G. 1994. Influence of surface properties of carbon black on the activity of adsorbed catalyses. *Carbon* 13: 1369-1375.

Stipp, S.L. & Hochella, M.F. 1991. Structure and bonding environments at the calcite surface at observed with X-ray photoelectron spectroscopy (XPS) and low energy electron diffraction (LEED). *Geochim. Cosmochim. Acta* 55: 1723-1736.

Wolf, A.R. & Ferris, F.G. 1995. Spectroscopy speciation and qualification of metals associated with epilithic biofilms in a watershed impacted by acid mine drainage. In *Mining and the Environment*, Hynes, T.P. & Blanchette, M.C. (Eds.), Sudbury 95, CANMET: 805-811.

Xiao, S.J., Textor, M., Spencer, N.D., Wieland, M., Keller, B. & Sigrist, H. 1997. Effect of biofilms structures in oxygen distribution and mass transport using XPS. *J. Mater. Sci. Mater. Med*. 8: 867-875.

Fathul Karim Sahrani
Pusat Pengajian Sains Sekitaran dan Sumber Alam
Fakulti Sains dan Teknologi
Universiti Kebangsaan Malaysia
43600 Bangi, Selangor Darul Ehsan
Malaysia

Madzlan Abd. Aziz, Zaharah Ibrahim & Adibah Yahya
Jabatan Kimia / Biologi, Fakulti Sains
Universiti Teknologi Malaysia
81310 Skudai, Johor Darul Takzim
Malaysia

Received : 25 July 2007
Accepted : 25 September 2007